Managing Charge Balance and Triplet Excitons to Achieve High-Power-Efficiency Phosphorescent Organic Light-Emitting Diodes

Youtian Tao,[†] Qiang Wang,[‡] Chuluo Yang,*[,†] Jingui Qin,[†] and Dongge Ma*[,‡]

Department of Chemistry, Hubei Key Lab on Organic and Polymeric Optoelectronic Materials, Wuhan University, Wuhan 430072, People's Republic of China, and State Key Laboratory of Polymer Physics and Chemistry, Changchun Institute of Applied Chemistry, Chinese Academy of Sciences, Changchun 130022, People's Republic of China

ABSTRACT High-efficiency phosphorescent organic light-emitting diodes (PhOLEDs) have been achieved by using an ortho-linked triphenylamine/oxadiazole hybrid, namely *p*-TPA-*o*-OXD, as host material. The high HOMO level of the compound (5.25 eV) can facilitate efficient hole injection from 1, 4-bis[(1-naphthylphenyl)amino]biphenyl (NPB) layer to the emissive layer. As a result, low driving voltages and high power efficiencies have been attained as compared to the carbazole-based hosts with lower HOMO levels and higher injection barriers under similar device structures. By introducing 1,3,5-tris(*N*-phenylbenzimidazol-2-yl)benzene (TPBI) to replace 2,9-dimethyl-4,7-diphenyl-1,10-phenanthroline (BCP)/tris(8-hydroxyquinoline)aluminum (Alq3) as hole blocking/electron transporting layer, followed by tuning the thicknesses of hole-transport NPB layer to manipulate the charge balance, high-efficiency PhOLEDs have been achieved, with maximum current efficiency/power efficiency/external quantum efficiency of 85.7 cd/A/99.7 lm/W/22.2% for green $(ppy)_2Ir(acac)$-based devices, 55.2 cd/A/64.2 lm/W/19.0% for yellow $(fbi)_2Ir(acac)$-based devices, and 11.4 cd/A/11.8 lm/W/14.8% for deep red $(piq)_2Ir(acac)$-based devices. By inserting 10 nm of *p*-TPA-*o*-OXD as self-triplet exciton blocking layer between hole transporting and emissive layer to confine triplet excitons, device performances have been further improved in green PhOLED, with peak current efficiency/power efficiency/external quantum efficiency of 90.0 cd/A/97.7 lm/W/23.5%.

KEYWORDS: phosphorescent organic light-emitting diodes • host • charge balance • triplet energy • energy level

INTRODUCTION

Since the report of organic light-emitting diodes (OLED) based on phosphorescent emitters, there has been intensive interests in these devices because they can approach a 100% internal quantum efficiency theoretically by utilizing both singlet and triplet excitons (1−8). Therefore, much higher external quantum efficiency (EQE) can be achieved than conventional fluorescent OLEDs (1−3). Generally, for high electrophosphorescent efficiency to be achieved, heavy metal complexes of phosphors have to be dispersed into host materials to reduce competitive factors such as concentration quenching and triplet−triplet annihilation, and thus host materials are of equal importance with the phosphor guests (1, 2). It is desirable that the host materials have a large enough band gap for effective energy transfer to guest, and good carrier transport properties for a balanced carriers recombination in emitting layer, as well as energy-level matching with neighboring layers for effective charge injection. However, a trade-off is also required between the energy gap and the highest occupied molecular orbital (HOMO) and lowest unoccupied molecular orbital (LUMO) of the host. A high triplet energy generally signifies a large electrical band gap, i.e., a low-lying HOMO and/or high-lying LUMO level, which are not easy to match the energy levels of adjacent layers (9); from this view, to design host for green to red phosphors, a large energy gap is not indispensable; instead, a relatively narrow energy gap (e.g., < 3 eV) and matched HOMO and LUMO levels with adjacent layers are preferable.

Carbazole-containing compounds have been widely used as host materials in PhOLEDs because of their large triplet energies and good hole-transporting ability (10−13). For example, 4, 4′-*N*, *N*′-dicarbazole-biphenyl (CBP) is a prominent host for green and red triplet emitters (4, 14−17). Unfortunately, CBP host is prone to crystallize for its rather low glass transition temperature (62 °C) (11). Additionally, the driving voltages of CBP based device are usually rather high because of the large difference in HOMO level between CBP and adjacent hole transporting layer (18, 19).

In our previous work (12), we reported a maximum current efficiency ($\eta_{c\ max}$) of 77.9 cd/A for green *fac*-tris(2-phenylpyridine)iridium(III) [$Ir(ppy)_3$] based device by using an ortho-linked carbazole/oxadiazole hybrid molecule as bipolar host. However, the maximum power efficiency ($\eta_{p\ max}$) of 59.3 lm/W of this device is not very satisfying. This may relate to the large hole-injection barrier caused by the low HOMO level (5.55 eV) of this host. To make the OLED

* Corresponding author. E-mail: clyang@whu.edu.cn (C.Y.); mdg1014@ciac.jl.cn (D.M.).
Received for review June 7, 2010 and accepted August 23, 2010
[†] Wuhan University.
[‡] Chinese Academy of Sciences.
DOI: 10.1021/am100495g

Scheme 1. Chemical Structures of the Host *p*-TPA-*o*-OXD and the Guests Used in This Work

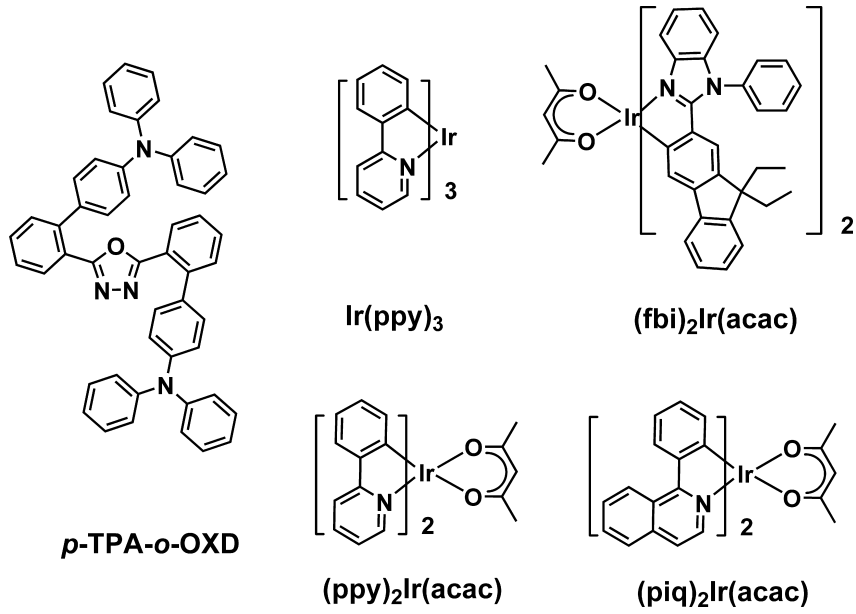

products more energy efficient and with longer device lifetimes, high power efficiency device is demanded. Herein, we report the results on improving the power efficiencies of green, yellow and deep red PhOLEDs by using ortho-linked triphenylamine/oxadiazole hybrid as bipolar host. The reason we choose triphenylamine (TPA) to replace carbazole lies in triphenylamine having a high triplet energy and good hole-transporting ability like carbazole; moreover, most triphenylamine compounds have higher HOMO levels (ca. 5.3 eV) than do carbazole derivatives, which is close to the work function of ITO or widely used hole transporting material NPB, and thus allow efficient hole injection (20, 21). We will also report the optimization of device structures by introducing a layer of hole-blocking/electron-transporting 1,3,5-tris(*N*-phenylbenzimidazol-2-yl)benzene (TPBI), followed by tuning the thicknesses of hole-transport NPB layer to manipulate the charge balance, or by inserting a thin layer of *p*-TPA-*o*-OXD between hole-transport and emissive layer as self-triplet exciton blocking layer to confine the triplet excitons.

EXPERIMENTAL SECTION

Materials. MoO_3 was commercially available from Alfa Aesar; NPB (1,4-bis(1-naphthylphenylamino)-biphenyl), Alq3 (tris(8-hydroxyquinoline)aluminum), and TPBI (1,3,5-tris(*N*-phenylbenzimidazol-2-yl)benzene) were purchased from eRay Optoelectronic Technology; BCP (2,9-dimethyl-4,7-diphenyl-1,10-phenanthroline) was purchased from Sigma-Aldrich; $Ir(ppy)_3$ was purchased from eLight Corporation. Bis(2-phenylpyridinato)iridium(III) acetylacetonate [$(ppy)_2Ir(acac)$] (4), bis(2-(9,9-diethyl-9*H*-fluoren-2-yl)-1-phenyl-1*H*-benzoimidazol-N,C3)-iridium(acetylacetonate) [$(fbi)_2Ir(acac)$] (17) and bis(1-phenylisoquinolinato)(acetylacetonate)iridium [$(piq)_2Ir(acac)$] (14) were synthesized according to literature reported procedures. 2′,2″-(1,3,4-oxadiazole-2,5-diyl)bis(*N*,*N*-diphenylbiphenyl-4-amine) (*p*-TPA-*o*-OXD) was prepared according to our previous report (22).

Device Fabrication and Measurement. Commercial indium tin oxide (ITO) coated glass with sheet resistance of 10 Ω/sq was used as the starting substrates. Before device fabrication, the ITO glass substrates were precleaned through ultrasonic bath in ethanol and acetone, respectively, washed by special active detergent, dried at 120 °C, and then treated by oxygen plasma for 2 min. All layers were grown by thermal evaporation in a high vacuum system with pressure of less than 5×10^{-4} Pa without breaking the vacuum. In the deposition of the doping layers, deposition rates of both host and guest were controlled with their correspondingly independent quartz crystal oscillators. The evaporation rates were monitored by frequency counter, and calibrated by Dektak 6 M Profiler (Veeco). The overlap between ITO and Al electrodes was 4×4 mm^2 as the active emissive area of the devices. Current density−voltage-brightness characteristics were measured by using a Keithley source measurement unit (Keithley 2400 and Keithley 2000) with a calibrated silicon photodiode. The EL spectra were measured by JY SPEX CCD3000 spectrometer. Four testing points for each device were made under the same experimental conditions. All the measurements were carried out in ambient conditions without encapsulation soon after the devices being taken out of the vacuum. The medial experimental data were selected among the four testing points.

RESULTS AND DISCUSSION

Using *p*-TPA-*o*-OXD as host material, we first fabricated device A_1 by using the most widely reported green triplet emitter $Ir(ppy)_3$, with the device configuration of ITO/MoO_3 (10 nm)/NPB (80 nm)/*p*-TPA-*o*-OXD: $Ir(ppy)_3$ (11 wt %, 20 nm)/BCP (10 nm)/Alq3 (30 nm)/LiF (1 nm)/Al(100 nm), where NPB and Alq3 are used as the hole- and electron-transporting layer, respectively; BCP is used as hole- and exciton-blocking layer; MoO_3 (23) and LiF serve as hole- and electron-injecting layer, respectively. The current density−voltage−luminance characteristics and external quantum efficiency versus current density curves are shown in Figure 1, and all EL data are summarized in Table 1. The device achieved excellent performance, with a maximum current efficiency of 79.0 cd/A and a maximum external quantum of 22.0%, which are higher than our previously reported similar devices using *o*-CzOXD as host (77.9 cd/A and 20.2%) (12), and even higher than those p−i−n double

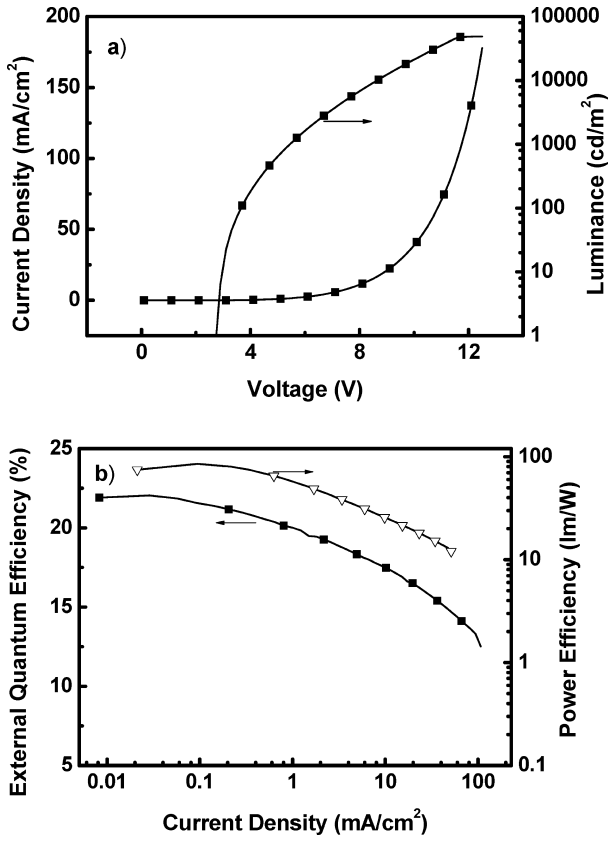

FIGURE 1. (a) Current density−voltage−luminance characteristics and (b) external quantum efficiency/power efficiency versus current density curves for devices A_1.

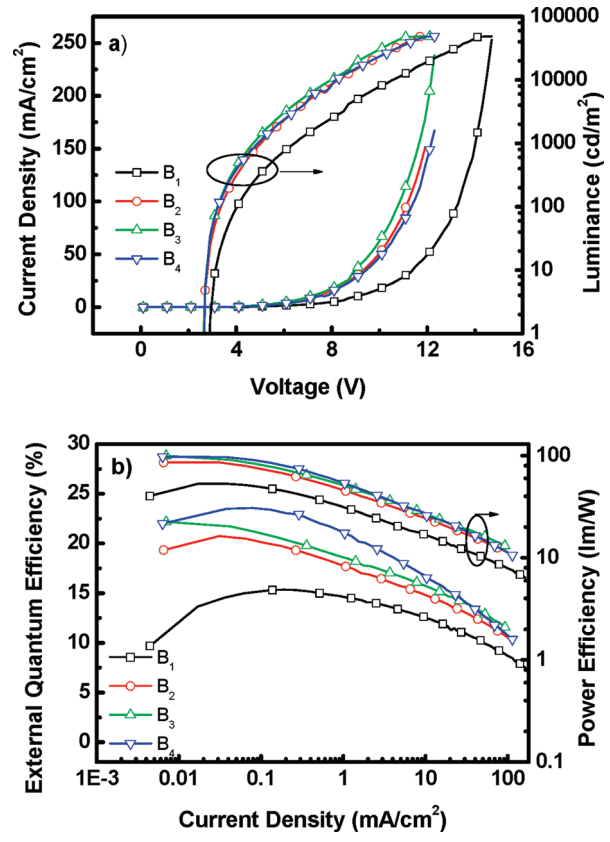

FIGURE 2. (a) Current density−voltage−luminance characteristics and (b) external quantum efficiency/power efficiency versus current density curves for green $(ppy)_2Ir(acac)$ based devices B_1−B_4.

emissive layer devices (24). It is noteworthy that device A_1 displays lower turn-on voltage of 2.9 V than those similar devices with carbazole-based host materials, such as *o*-CzOXD (3.1 V for $Ir(ppy)_3$) and CBP (3.3 V for $Ir(ppy)_3$ (12). The low driving voltage should be attributed to the matched HOMO levels between NPB (5.4 eV) and *p*-TPA-*o*-OXD host (5.25 eV). Accordingly, the maximum power efficiency remarkably rises to 85.0 lm/W as compared to the similar device using *o*-CzOXD as host (59.4 lm/W) (12).

To investigate the universal applicability of the host material, we fabricated devices B−D based on diverse phosphorescent dopants [green $(ppy)_2Ir(acac)$ for B, yellow $(fbi)_2Ir(acac)$ for C, and deep red $(piq)_2Ir(acac)$ for D]. The doping concentrations for the emitters were 9, 7, and 6 wt %, respectively. For B_1−D_1, the device configurations are similar to A_1 with BCP/Alq3 as hole-blocking and electron-transporting layer; for B_2−D_2, a 40 nm thick TPBI layer is used to replace BCP/Alq3 to simplify the device structure and improve the EL performance; for B_3−D_3, NPB thicknesses are reduced to 70 nm to get a charge balance.

For green $(ppy)_2Ir(acac)$-based device B (Figure 2a), B_1 with BCP/Alq3 as hole-blocking and electron-transporting layer show higher operating voltage than TPBI-based B_2 and

Table 1. EL Data of Devices A−D

	dopant	NPB (nm)	HBL/ETL	$V_{turn\text{-}on}$ (V)	L_{max}(cd/m^2)[a], voltages (V)	$\eta_{c.max}$[b] (cd/A)	$\eta_{p.max}$[c] (lm/W)	$\eta_{ext.}$ (%)[d]	CIE
A_1	$Ir(ppy)_3$	80	BCP/Alq3	2.9	48815, 12.5	79.9	85.0	22.0, 19.4, 16.6	0.30, 0.63
B_1	$(ppy)_2Ir(acac)$	80	BCP/Alq3	2.9	48501, 14.5	59.0	53.2	15.3, 14.1, 11.5	0.34. 0.62
B_2		80	TPBI	2.7	48208, 11.9	79.1	85.8	20.7, 17.0, 13.8	0.35, 0.61
B_3		70		2.7	48613, 11.7	85.7	99.7	22.2, 18.2, 14.7	0.33, 0.63
B_4		70		2.7	48513, 12.3	90.0	97.7	23.5, 20.7, 15.3	0.35, 0.61
C_1	$(fbi)_2Ir$ (acac)	80	BCP/Alq3	2.9	48314, 13.9	38.8	42.0	13.5, 11.9, 9.4	0.51, 0.48
C_2		80	TPBI	2.7	46836, 13.1	52.5	61.1	17.9, 14.0, 11.3	0.51, 0.49
C_3		70		2.7	48548, 13.1	55.2	64.2	19.0, 13.3, 10.7	0.51, 0.49
D_1	$(piq)_2Ir$ (acac)	80	BCP/Alq3	3.1	24416, 14.9	11.3	8.2	14.2, 12.2, 8.1	0.68. 0.32
D_2		80	TPBI	2.7	24573, 13.9	11.5	11.8	14.4, 12.1, 7.6	0.68, 0.32
D_3		70		2.7	24740, 13.5	11.4	11.8	14.8, 12.0, 7.7	0.68, 0.32

[a] Maximum luminance. [b] Maximum current efficiency. [c] Maximum power efficiency. [d] Maximum external quantum efficiency (η_{ext}), η_{ext} at 1000 cd/m^2 and 10000 cd/m^2, respectively.

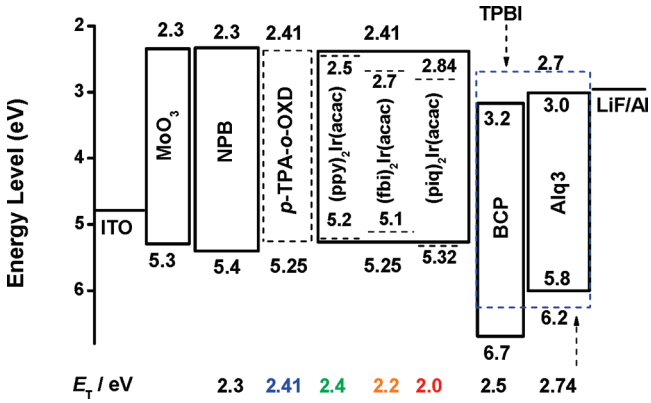

FIGURE 3. Energy level diagram of HOMO and LUMO levels (relative to vacuum level) for materials investigated in this work.

B_3. The voltages at luminance of 1000 and 10 000 cd/m^2 are 6.5 and 10.5 V for device B_1, respectively, whereas those are 5.0 and 8.3 V for device B_2 and 4.7 and 8.0 V for B_3. Moreover, the TPBI based devices exhibit significantly enhanced EL efficiencies. As shown in Table 1, a 35% enhancement of maximum external quantum efficiency is observed in B_2 (20.7%) compared to B_1 (15.3%). This can be explained as follows: (i) because the hole mobility of NPB is about two orders higher than the electron mobility of Alq3 (25−27), the introduction of TPBI with higher electron mobility over BCP/Alq3 can facilitate the electron currents (28), which consequently decrease the driving voltages and result in an improved charge balance; (ii) the higher triplet energy of TPBI (2.74 eV) over BCP (2.5 eV) (29, 30) can reduce nonradiative recombination through energy transfer from the emissive excited state of $(ppy)_2Ir(acac)$ to the triplet state of exciton blocking material, and thus confine the triplet excitons inside the emitting layer; (iii) as demonstrated in the energy diagram of Figure 3, holes could be easily injected to the emitting layer (EML) because there is no hole-injection barrier from NPB to *p*-TPA-*o*-OXD host, whereas the higher LUMO level of TPBI (2.7 eV) (31) over BCP (3.2 eV) (29) can facilitate the electron injection from hole-blocking layer (HBL) to EML, which accordingly lead to an improved charge balance; (iv) thick buffer layer generally causes high driving voltages (25). The 80 nm NPB layer in devices B_1 and B_2 is significantly thicker than that of 30−40 nm in most reported devices (1, 2). Moreover, the enhancement of electron current caused by the introduction of TPBI requires the increase in hole current simultaneously for charge balance. Therefore, the best EL performance was achieved in the doubly optimized device structure of B_3.

It is important to confine excitons in EML to increase the recombination efficiency of holes and electrons by blocking both charge carriers and excitons diffusion out of emissive layer. Because the triplet energy (E_T) of NPB (2.3 eV) (29, 30) is not high enough to block triplet excitons of green emitter $(ppy)_2Ir(acac)$ (E_T: 2.41 eV) (32), devices B_4 with the configuration of ITO/MoO_3 (10 nm)/NPB (70 nm)/*p*-TPA-*o*-OXD (10 nm)/*p*-TPA-*o*-OXD:$(ppy)_2Ir(acac)$ (9 wt %, 20 nm)/TPBI (40 nm)/LiF (1 nm)/Al(100 nm) was fabricated to further improve the device performance, in which a thin layer of *p*-TPA-*o*-OXD with higher E_T (2.41 eV) over NPB was inserted

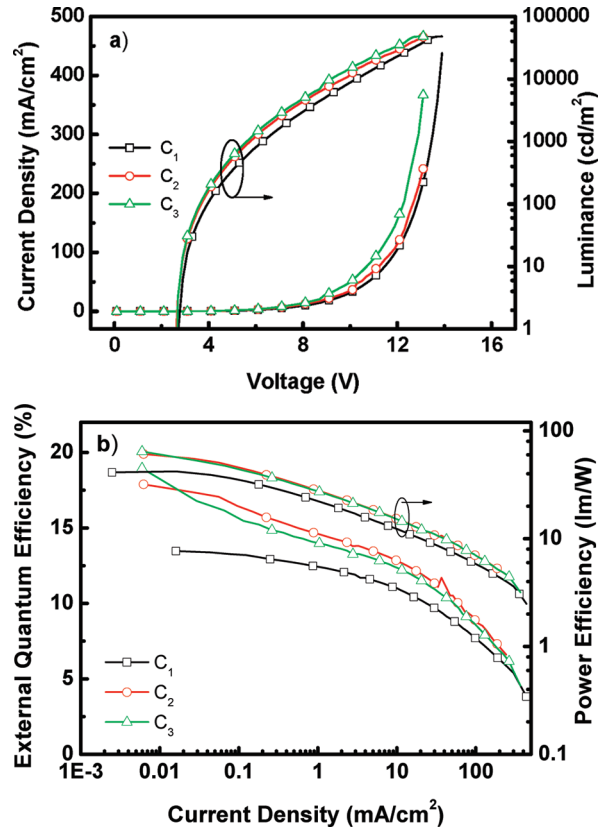

FIGURE 4. (a) Current density−voltage−luminance characteristics and (b) external quantum efficiency/power efficiency versus current density curves for yellow $(fbi)_2Ir(acac)$-based devices C_1−C_3.

between the NPB and EML to function as both hole transporting and triplet exciton blocking layer (EBL). As shown in Figure 2a, B_4 with 70 nm of NPB and 10 nm of *p*-TPA-*o*-OXD exhibits almost identical *J*−*V* characteristics to B_2 with 80 nm of NPB, suggesting the good hole-transport ability of *p*-TPA-*o*-OXD. As expected, device B_4 with the introduction of a thin layer of self-triplet exciton confining layer displays the highest EL efficiency among the four devices (B_1−B_4), with a maximum current efficiency of 90.0 cd/A, a maximum power efficiency of 97.7 lm/W and a maximum external quantum efficiency of 23.5%, respectively. We note that the device performance is the highest among the devices using $(ppy)_2Ir(acac)$ as phosphor dopant under similar device structures (3a), and even comparative to top-emission *n*-Si:Au-based n-doping PhOLEDs (85 ± 9 cd/A, 80 ± 8 lm/W) (33).

Similar trends can be observed in the yellow emissive devices C_1−C_3 (Figure 4). Device C_1 achieves a maximum current efficiency of 38.8 cd/A, which is comparable to previously reported CBP host (~37 cd/A). Noticeably, its maximum power efficiency (42 lm/W) is 1.5 times higher than that of CBP (~27 lm/W) hosted device (17). Device C_2 attains a maximum current efficiency of 52.5 cd/A, a maximum power efficiency of 61.1 lm/W, and a maximum external quantum efficiency of 17.9%, and these values are further enhanced to 55.2 cd/A, 64.2 lm/W, and 19.0% for Device C_3 with reduced NPB thickness. The significant enhancement of EL efficiency for TPBI-based devices C_2 and C_3 as compared to BCP/Alq3-based device C_1 can be at-

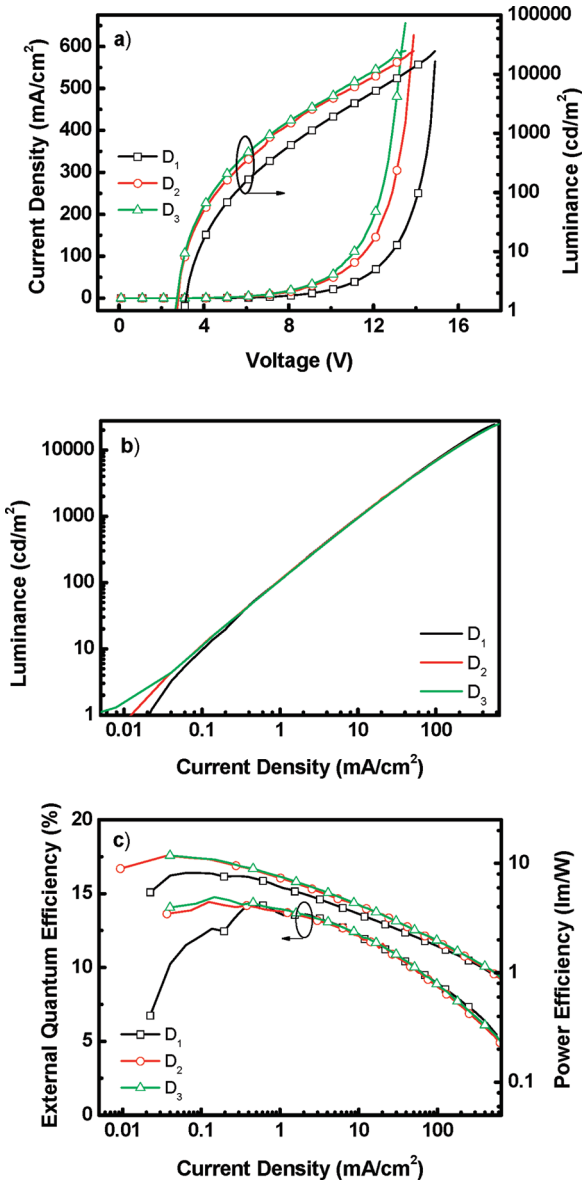

FIGURE 5. (a) Current density−voltage−luminance characteristics, (b) current density−luminance curves, and (c) external quantum efficiency/power efficiency versus current density curves for deep red $(piq)_2Ir(acac)$-based devices D_1−D_3.

tributed to the increase in electron current and improvement in electron injection from the HBL/ETL side to the emissive layer.

As reported previously, red PhOLEDs with the most widely used CBP host usually need high driving voltages because the poor energy matching between CBP and adjacent hole- and electron-transporting layers can result in insufficient and/or unbalanced injection of holes and electrons (19). Thus it is of significance to choose appropriate host material with matching energy levels for red electrophosphorescence. Herein, *p*-TPA-*o*-OXD host with a narrow energy gap (2.84 eV) could be a desirable candidate. Devices D_2 and D_3 display higher current density and luminance than device D_1 at the same operating voltages (Figure 5a); however, their current density−luminance curves (Figure 5b) are almost the same, therefore the three red devices show almost equivalent current and external quantum efficiency.

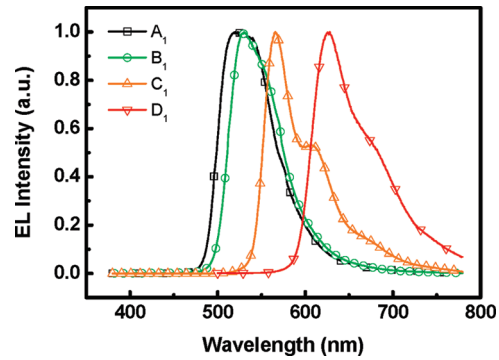

FIGURE 6. Electroluminescence spectra of devices A_1−D_1 with *p*-TPA-*o*-OXD as host material.

Device D_1 shows a turn-on voltage of 3.1 V, which is significantly lower than that of CBP hosted device (5.3 V) (12). This value is further reduced to 2.7 V for devices D_2 and D_3 using TPBI as hole-blocking and electron-transporting layer; in consequence, the power efficiencies of devices D_2 and D_3 are enhanced by 11.8 lm/W from 8.2 lm/W in D_1 (Figure 5c).

CONCLUSION

In conclusion, we have demonstrated that an ortho-linked triphenylamine/oxadiazole hybrid (*p*-TPA-*o*-OXD) with narrow energy gap can be used as efficient host material for green, yellow, and deep red phosphorescent OLEDs. Low driving voltages and high power efficiencies have been achieved because of its matched HOMO level with adjacent hole-transport NPB layer, which facilitate the efficient hole injection from NPB to the emissive layer. Furthermore, through using a single TPBI layer to replace generally used BCP/Alq3, followed by reducing the hole-transport NPB layer thicknesses, we can substantially improve power efficiencies, with peak power efficiencies enhanced by 99.7 lm/W from 53.2 lm/W for $(ppy)_2Ir(acac)$-based devices, 64.2 lm/W from 53.2 lm/W for yellow emissive $(fbi)_2Ir(acac)$-based devices, and 11.8 lm/W from 8.2 lm/W for red emissive $(piq)_2Ir(acac)$-based devices. The enhanced EL performance is attributed to improved charge balance and confinement of triplet excitons in the emissive layer.

Acknowledgment. We thank the National Natural Science Foundation of China (Project 90922020, 50773057, and 20621401) and the National Basic Research Program of China (973 Program-2009CB623602, 2009CB930603) for financial support.

REFERENCES AND NOTES

(1) Baldo, M. A.; O'Brien, D. F.; You, Y.; Shoustikov, A.; Sibley, S.; Thompson, M. E.; Forrest, S. R. *Nature* **1998**, *395*, 151.
(2) Baldo, M. A.; Lamansky, S. P.; Burrows, E.; Thompson, M. E.; Forrest, S. R. *Appl. Phys. Lett.* **1999**, *75*, 4.
(3) (a) Adachi, C.; Baldo, M. A.; Thompson, M. E.; Forrest, S. R. *J. Appl. Phys.* **2001**, *90*, 5048. (b) Tao, Y.; Wang, Q.; Ao, L.; Zhong, C.; Yang, C.; Qin, J.; Ma, D. *J. Phys. Chem. C* **2009**, *114*, 601.
(4) Lamansky, S.; Djurovich, P.; Murphy, D.; Abdel-Razzaq, F.; Lee, H. E.; Adachi, C.; Buttows, P. E.; Forrest, S. R.; Thompson, M. E. *J. Am. Chem. Soc.* **2001**, *123*, 4304.
(5) Watanabe, S.; Ide, N.; Kido, J. *Jpn. J. Appl. Phys.* **2007**, *46*, 1186.
(6) Tanaka, D.; Sasabe, H.; Li, Y. J.; Su, S. J.; Takeda, T.; Kido, J. *Jpn. J. Appl. Phys.* **2007**, *46*, L10.

(7) Ikai, M.; Tokito, S.; Sakamoto, Y.; Suzuki, T.; Taga, Y. *Appl. Phys. Lett.* **2001**, *79*, 156.
(8) Chien, C. H.; Hsu, F. M.; Shu, C. F.; Chi, Y. *Org. Electron.* **2009**, *10*, 871.
(9) Gao, Z. Q.; Luo, M.; Sun, X. H.; Tam, H. L.; Wong, M. S.; Mi, B. X.; Xia, P. F.; Cheah, K. W.; Chen, C. H. *Adv. Mater.* **2009**, *21*, 688.
(10) Tsai, M.-H.; Lin, H.-W.; Su, H.-C.; Ke, T.-H.; Wu, C.-c.; Fang, F.-C.; Liao, Y.-L.; Wong, K.-T.; Wu, C.-I. *Adv. Mater.* **2006**, *18*, 1216.
(11) Tsai, M.-H.; Hong, Y.-H.; Chang, C.-H.; Su, H.-C.; Wu, C.-C.; Matoliukstyte, A.; Simokaitiene, J.; Grigalevicius, S.; Grazulevicius, J. V.; Hsu, C.-P. *Adv. Mater.* **2007**, *19*, 862.
(12) (a) Tao, Y.; Wang, Q.; Yang, C.; Wang, Q.; Zhang, Z.; Zou, T.; Qin, J.; Ma, D. *Angew. Chem., Int. Ed.* **2008**, *47*, 8104. (b) Tao, Y.; Wang, Q.; Yang, C.; Zhong, C.; Zhang, K.; Qin, J.; Ma, D. *Adv. Funct. Mater.* **2010**, *20*, 304.
(13) Hsu, F. M.; Chien, C. H.; Shih, P. I.; Shu, C. F. *Chem. Mater.* **2009**, *21*, 1017.
(14) Li, C.-L.; Su, Y.-J.; Tao, Y.-T.; Chou, P.-T.; Chien, C.-H.; Cheng, C.-C.; Liu, R.-S. *Adv. Funct. Mater.* **2005**, *15*, 387.
(15) Yang, C.; Zhang, X.; You, H.; Zhu, L. Y.; Chen, L.; Zhu, L. N.; Tao, Y. T.; Ma, D. G.; Shuai, Z.; Qin, J. *Adv. Funct. Mater.* **2007**, *17*, 651.
(16) Tsuboyama, A.; Iwawaki, H.; Furugori, M.; Mukaide, T.; Kamatani, J.; Igawa, S.; Moriyama, T.; Miura, S.; Takiguchi, T.; Okada, S.; Hoshino, M.; Ueno, K. *J. Am. Chem. Soc.* **2003**, *125*, 12971.
(17) Huang, W. S.; Lin, J. T.; Chien, C. H.; Tao, Y. T.; Sun, S. S.; Wen, Y. S. *Chem. Mater.* **2004**, *16*, 2480.
(18) Jeon, S. O.; Yook, K. S.; Joo, C. W.; Son, H. S.; Jang, S. E.; Lee, J. Y. *Org. Electron.* **2009**, *10*, 998.
(19) Kanno, H.; Ishikawa, K.; Nishio, Y.; Endo, A.; Adachi, C.; Shibata, K. *Appl. Phys. Lett.* **2007**, *90*, 123509.
(20) Tao, L.; Li, J.; Yu, Y.; Jiang, Y.; Zhou, C.-S.; Lee, S.-T.; Zhang, X.; Kwon, O. *Chem. Mater.* **2009**, *21*, 1284.
(21) Shih, P.-I.; Chien, C.-H.; Wu, F.-I.; Shu, C.-F. *Adv. Funt. Mater.* **2007**, *17*, 3514.
(22) Tao, Y.; Wang, Q.; Shang, Y.; Yang, C.; Qin, J.; Ma, D.; Shuai, Z. *Chem. Commun.* **2009**, 77.
(23) You, H.; Dai, Y.; Zhang, Z.; Ma, D. *J. Appl. Phys.* **2007**, *101*, 026105.
(24) He, G.; Pfeiffer, M.; Leo, K.; Hofmann, M.; Birnstock, J.; Pudzich, R.; Salbeck, J. *Appl. Phys. Lett.* **2004**, *85*, 3911.
(25) Tong, Q.-X.; Lai, S.-L.; Chan, M.-Y.; Lai, K.-H.; Tang, J.-X.; Kwong, H.-L.; Lee, C.-S.; Lee, S.-T. *Chem. Mater.* **2007**, *19*, 5851.
(26) Aziz, H.; Popovic, Z. *Appl. Phys. Lett.* **2002**, *80*, 2180.
(27) Vanslyke, S. A.; Chen, C. H.; Tang, C. W. *Appl. Phys. Lett.* **1996**, *69*, 2160.
(28) Li, Y. Q.; Fung, M. K.; Xie, Z.; Lee, S.-T.; Hung, L.-S.; Shi, J. *Adv. Mater.* **2002**, *14*, 1317.
(29) Adamovich, V. I.; Cordero, S. R.; Djurovich, P. I.; Tamayo, A.; Thompson, M. E.; D'Andrade, B. W.; Forrest, S. R. *Org. Electron.* **2003**, *4*, 77.
(30) Kondakova, M. E.; Pawlik, T. D.; Young, R. H.; Giesen, D. J.; Kondakov, D. Y.; Brown, C. T.; Deaton, J. C.; Lenhard, J. R.; Klubek, K. P. *J. Appl. Phys.* **2008**, *104*, 094501.
(31) Tao, Y. T.; Balasubramaniam, E.; Danel, A.; Tomasik, P. *Appl. Phys. Lett.* **2000**, *77*, 933.
(32) Chen, Y.-C.; Huang, G.-S.; Hsiao, C.-C.; Chen, S.-A. *J. Am. Chem. Soc.* **2006**, *128*, 8549.
(33) Li, Y. Z.; Xu, W. J.; Ran, G. Z.; Qin, G. G. *Appl. Phys. Lett.* **2009**, *95*, 033307.

AM100495G